Steady-State and Laser Photolysis Studies of a Triarylmethane-Type Resin in Solution. Formation and Reactivity of Stable Radical Sites

Shuichi Hashimoto,* Etsuko Hoshino, Naomi Kato, and Michiya Ota

Chemistry Department, Gunma College of Technology, 580 Toriba-machi, Gunma 371, Japan

Hiroya Kakegawa

Advanced Technology Center, Osaka Gas Company, 5-11-61, Konohana-ku, Osaka 554, Japan

Received April 11, 1991; Revised Manuscript Received November 13, 1991

ABSTRACT: The formation of a stable free radical, possibly a triarylmethyl-type radical site (radical A), is observed on photoirradiation of a triarylmethane-type resin synthesized from pyrene and benzaldehyde (Py–BA resin) in CH_2Cl_2 solutions. The extremely slow decay of radical A in the dark is observed to proceed via second-order kinetics, which suggests the occurrence of a bimolecular disproportionation reaction, while the reaction tends to be first-order under continuous irradiation. The formation yield, the stability, and the decay mechanism of radical A are highly dependent on the solvent. In cyclohexane and CCl_4, radical A is unstable and its yield is low. In CH_2Cl_2 and in benzene, radical A is fairly stable but the yield is significantly higher in CH_2Cl_2. In CCl_4, radical A decays by reacting with solvent radicals generated in parallel by CCl_4 quenching of the Py–BA excited states. In order to clarify the formation and decay mechanism of radical A, *p*-benzoquinone (BQ) was added to the CH_2Cl_2 and benzene solutions. In that case, the decay of radical A results in a triarylmethyl-type cation in CH_2Cl_2, while, in benzene, the parent molecule is recovered in a >98% yield.

Introduction

Triarylmethane-type resins recently synthesized by condensation between aromatic hydrocarbons and aromatic aldehydes have attracted much attention because of their application to thermoresist resins[1] and also because of their potential as organic ferromagnets.[2]

The characteristic properties of these resins are attributable to the presence of a methine carbon center surrounded by three aromatic moieties. This is different from classical phenol resins which have methylene groups connected to two aromatics. The methine H is highly reactive toward hydrogen-abstracting species.[3] Hence, the triarylmethane-type resins are expected to undergo dehydrogenation without great difficulty, resulting in the formation of triarylmethyl-type radicals. Previous investigations[2] revealed that photoirradiation of the resins in the presence of *p*-benzoquinone produces stable free radicals, which were detected by ESR. Furthermore, such a resin powder shows a weak magnetic hysteresis. However, no detailed study on the origin of these radicals has yet been undertaken.

In order to clarify this aspect, we have carried out the characterization of these radicals and investigated their reactivity by optical absorption (both steady-state and transient) and by ESR measurements.

Experimental Section

Materials. A triarylmethane-type pyrene–benzaldehyde (Py–BA) resin was synthesized and throughly purified according to the literature.[2] ^1H and ^{13}C NMR and IR spectra showed the presence of methine H atoms and the absence of both methylene groups and carbonyl groups. The presence of a slight amount of OH groups was confirmed as already described.[2] Field desorption mass spectra and GPC elution patterns show that the resin has an average molecular weight of 1700 and scarcely contains components of molecular weights less than 500 (i.e., one triarylmethane unit). The synthesized resin shows a wide molecular weight distribution. The resin is also expected to contain a considerable amount of structural isomers. Therefore, the model structure depicted in Figure 1 is adopted just for the purpose of discussion.

p-Benzoquinone (Tokyo Kasei; GR grade) was recrystallized three times from ethanol. Dichloromethane (Wako Pure Chemicals; GR) and benzene (Wako; HPLC grade) were purified by standard procedures.[4] Cyclohexane (Wako; HPLC) and carbon tetrachloride (Wako; HPLC) were used as received.

Methods. Steady-state photolysis was carried out with a 500-W ultra-high-pressure Hg lamp (Ushio USH-500). The 365-nm light was isolated with a $CuSO_4$ solution and a Corning 7-54 and Toshiba UV-35 filters. The rate constants were determined from the average of at least five measurements.

Laser photolysis was carried out with a setup described previously.[5] Briefly, a N_2 laser (Usho Optics KN-1.2M; excitation wavelength, 337.1 nm; pulse width, 5 ns; energy, 5 mJ/pulse) was used for excitation. A 150-W Xe short arc lamp (Ushio UXL-150DS), whose intensity was increased 10–20 times with a pulse generator (Yamashita Denso: YXP-150W) when necessary, was used as a monitoring light. Beam intensities were monitored with a photomultiplier (PMT; Hamamatsu R-928; six stages) through a monochromator (Acton, SpectraPro 275). Signals from the PMT were fed into a digital storage oscilloscope (DSO; Gould 4072; 100 MHz, 400 Ms/s) through a back-off circuit.[6] All data were analyzed using a personal computer (NEC PC-9801DS) interfaced to the DSO. The time constant of the detection system was less than 50 ns.

Fluorescence decay was measured with a PMT (Hamamatsu 1P28; nine stages) and analyzed with a nonlinear least-squares method.[7]

A Shimazu UV-3101PC spectrophotometer and a Hitachi F-3010 spectrofluorimeter interfaced to a NEC personal computer were used for stationary measurements. The spectral response of the fluorescence instrument was corrected with fluorescence standards.[8] Fluorescence quantum yields were determined using as reference a quinine bisulfate solution in 0.1 N H_2SO_4 (0.54[9]).

Cyclic voltammetry was conducted with a Hokuto Denko HA-301 potentiostat and with a HB-104 function generator. ESR measurements were carried out on a JEOL JES-FE2XGS.

Sample solutions were deaerated by repeated freeze–pump–thaw cycles.

0024-9297/92/2225-1686$03.00/0

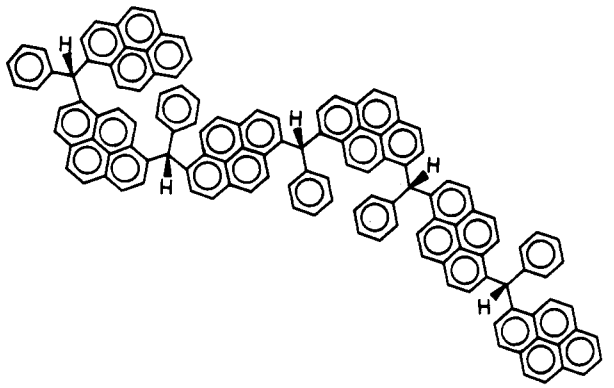

Figure 1. Structural model of Py–BA resin.

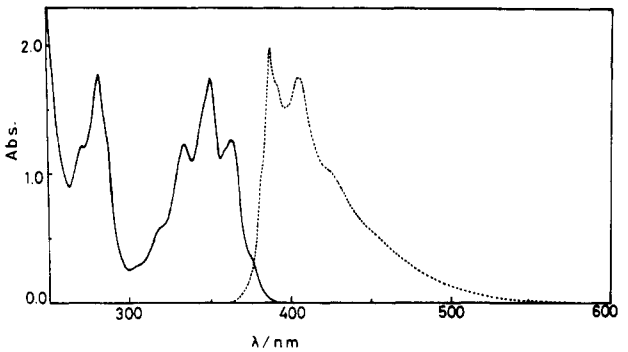

Figure 2. Absorption (—) and fluorescence (- - -) spectra of 1.0×10^{-2} g/L Py–BA resin.

Table I
Fluorescence Properties of Py–BA[a]

	C_6H_{12}	Bz	CH_2Cl_2	CCl_4
Φ_F	0.65	0.45	0.38	<0.01
τ_1, ns	31 ● 5	16 ± 3	12 ± 3	<5
τ_2, ns	105 ± 8	67 ± 7	49 ± 2	<5
α	0.38 ± 0.06	0.47 ± 0.01	0.38 ± 0.08	
η (20 °C)	1.0	0.65	0.44	0.97
EA, eV		-1.10	0.49	0.96
ϵ (20 °C)	2.02	2.27	8.93	2.24

[a] Φ_F, fluorescence quantum yield; τ_1, τ_2, fluorescence lifetime for the sum of two exponential approximations; α, preexponential factor for τ_1 (normalized to 1); η, viscosity (Cp); EA, electron affinity; ϵ, dielectric constant.

Results

1. Photoreactions of Py–BA in Solution. 1.1. Fluorescence Study. Figure 2 represents absorption and fluorescence spectra of a Py–BA resin in a CH_2Cl_2 solution. Both spectra are similar in transition energies to those of diluted pyrene solutions. No excimer band is observed even at significantly high concentrations. This suggests that the polymer structure is highly rigid and distorted and hence blocks the pyrene moieties from forming intramolecular and intermolecular excimers. In powder form, however, an excimer band is actually observed with a peak at 510 nm.

Table I lists the fluorescence quantum yields and fluorescence lifetimes of Py–BA measured in cyclohexane (C_6H_{12}), in benzene (Bz), in CH_2Cl_2, and in CCl_4. Fluorescence decay curves are fitted by the sum of two exponentials. Both the fluorescence quantum yield and the lifetime depend on the solvent, decreasing in the order of $CCl_4 > CH_2Cl_2 > Bz > C_6H_{12}$. This fluorescence quenching is due to the reactivity of the excited singlet state (S_1) as will be shown in the following section.

1.2. Transient Absorption. Transient absorption spectra measured in C_6H_{12}, Bz, CH_2Cl_2, and CCl_4 are shown in parts a–d of Figure 3. Both in C_6H_{12} and in Bz, broad transient spectra centered at 430 nm are observed. These absorption bands are very similar to that of the T–T absorption of pyrene in solution, which appears at 395 and 420 nm in *n*-hexane.[10] Furthermore, they are quenched efficiently by oxygen. Thus, these absorption bands can be assigned to the T–T absorption of Py–BA.

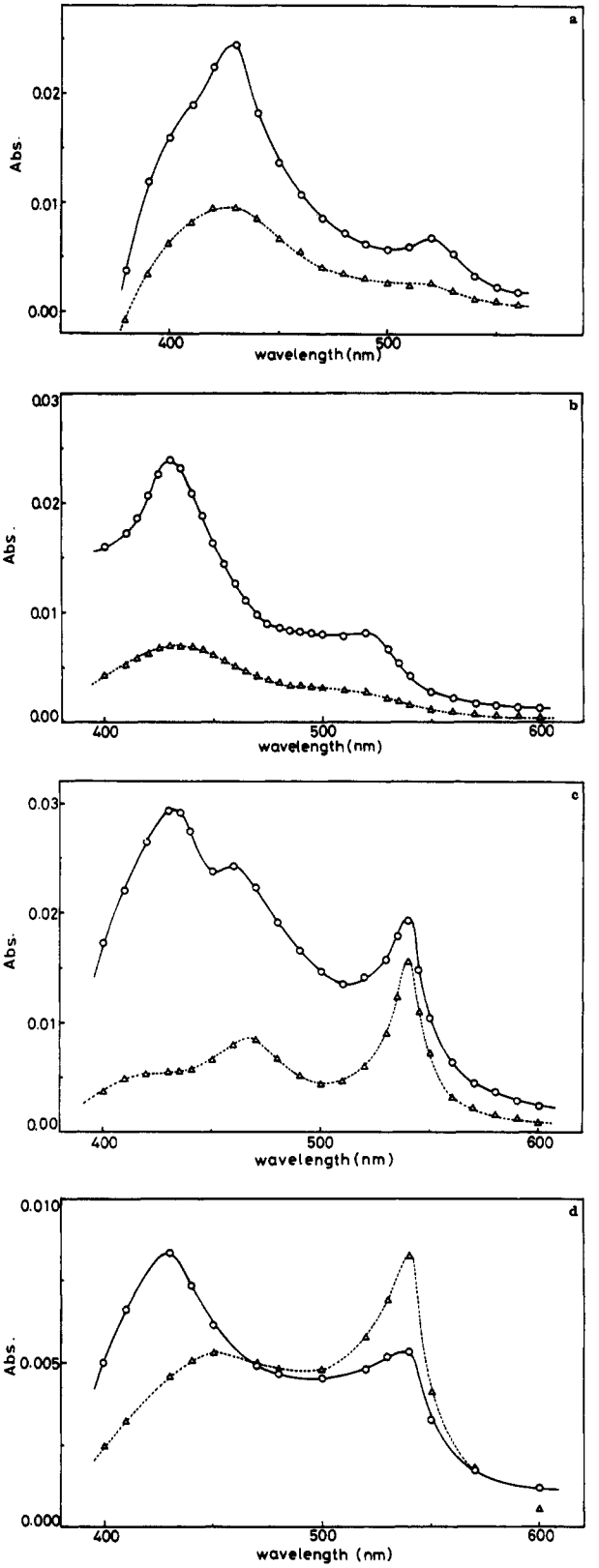

Figure 3. Transient absorption spectra of 1.5×10^{-2} g/L Py–BA. (a) In C_6H_{12}, delay: (○) 0 μs, (△) 450 μs. (b) In Bz, delay: (○) 0 μs, (△) 400 μs. (c) In CH_2Cl_2, delay: (○) 0 μs, (△) 450 μs. (d) In CCl_4, delay: (○) 0 μs, (△) 125 μs.

Table II
Relative Triplet Yield and Initial Half-Life ($\tau_{1/2}$) of the Triplet Decay

solvent	relative triplet yield[a]	$\tau_{1/2}$, μs
C_6H_{12}	1.00	190
Bz	0.87	190
CH_2Cl_2	1.26	45
CCl_4	1.10	14

[a] Relative absorbance at $t = 0$ μs at 430 nm after the contribution of radical A is subtracted (error 10%).

In Table II, comparison is made of the relative triplet yields (absorbance originating from the triplet at 430 nm) and the initial half-lifes ($\tau_{1/2}$) in different solvents. Transient species other than the triplet are not detectable in both solvents (i.e., in O_2-saturated solutions all signals disappear). The relative yield of the triplet appears to be slightly less (~10%) in Bz than in C_6H_{12}. The time-dependent decay profiles of the T–T absorption are similar ($\tau_{1/2}$ = 190 μs) in both solvents, showing a slight deviation from a simple first-order.

In CH_2Cl_2, on the other hand, the transient spectrum has new absorption bands at 540 and 460 nm in addition to the T–T absorption band. This band (referred to as band A) rises with the laser pulse and decays over a wide time range (microseconds to milliseconds to hours). As a result, after the triplet decay, the spectrum in CH_2Cl_2 becomes similar to the steady-state absorption spectrum. The decay of the T–T absorption in CH_2Cl_2 is faster ($\tau_{1/2}$ = 45 μs) than that observed in C_6H_{12} or Bz. Due to overlapping signals, we could not detect any rise in species A with the triplet decay. However, the contribution of the solvent quenching of the triplet state to the yield of A cannot be excluded.

In CCl_4, the spectrum after the laser pulse is also the superposition of the spectra of the triplet and that of A. In addition, band A grows at the expense of the triplet in the time range from 0 to 125 μs. Band A decays much faster in CCl_4 ($\tau_{1/2}$ = 2 ms) than in CH_2Cl_2.

1.3. Steady-State Irradiation. 1.3.1. Irradiation in CH_2Cl_2. On irradiation of Py–BA in deaerated CH_2Cl_2 with 365-nm light, absorption bands having peaks at 536, 460, and 390 nm appear with the concomitant disappearance of the parent absorption bands. Figure 4a shows this process as the difference spectrum with irradiation time. The new band evolving in Figure 4a has a close similarity to band A in the transient spectrum except for the 390-nm peak (this peak at 390 nm can be ascribed to another product due to its very different decay behavior). Accordingly, we assigned these bands, i.e., band A in the transient spectrum and the steady-state spectrum (peaks at 536 and 460 nm), to the same species. Further irradiation of the solution causes the decay of band A concomitantly with the development of a band around 400 nm (Figure 4b). The decay kinetics of A was measured at 536 nm and found to be first-order with a rate constant of (2.1 ± 0.4) × 10^{-4} s^{-1}. During this decay, further consumption of the parent bands was still observed. A change in the fluorescence spectrum was also measured: a new broad band centered at 510 nm appears at the expense of the parent band around 400 nm.

On the other hand, if the irradiation is discontinued before the 536-nm band has completely decayed and the sample solution is kept in the dark at room temperature, the decay at 536 nm is greatly slowed down and obeys second-order kinetics ($2k/\epsilon$ = (6.4 ± 1.8) × 10^{-5} s^{-1} cm) as shown in Figure 4c. The decay at 536 nm is compensated to some extent by the growth of the parent absorption bands. The growth kinetics of the parent compound at

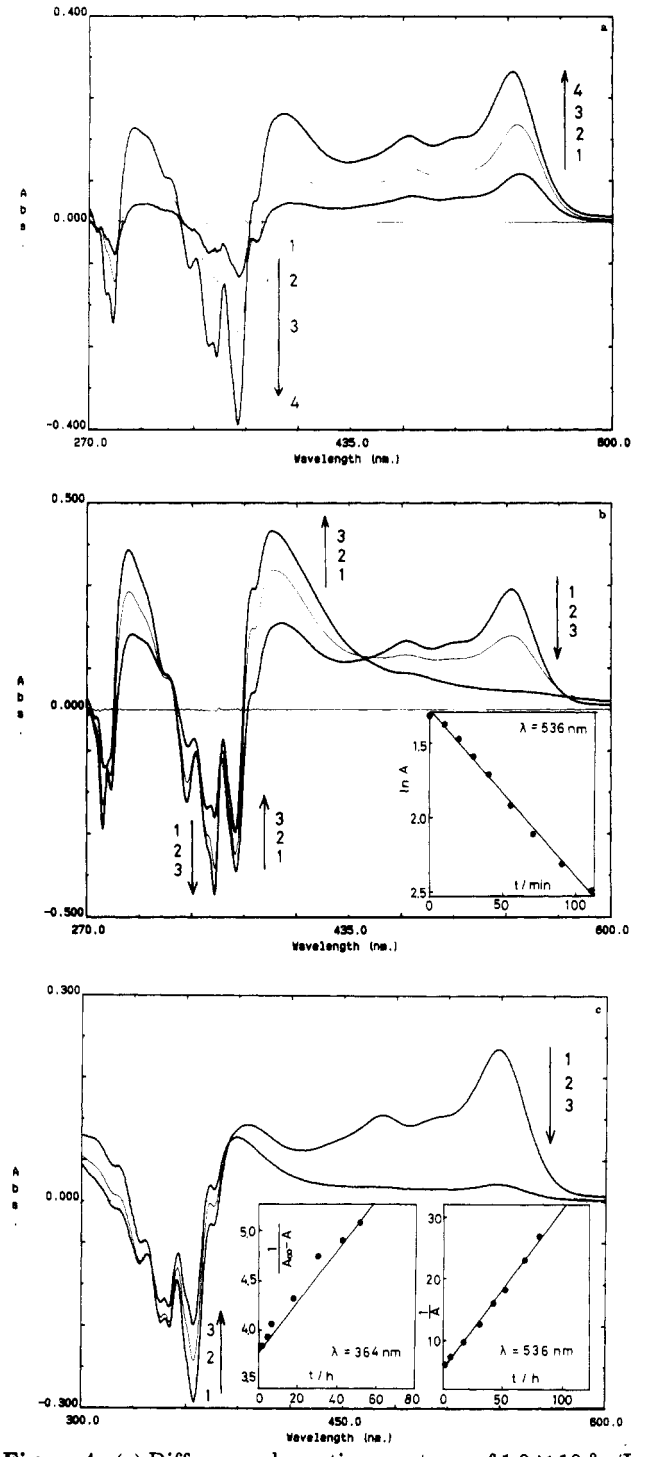

Figure 4. (a) Difference absorption spectrum of 1.0 × 10^{-2} g/L Py–BA with irradiation (λ_{ex} = 365 nm) time in CH_2Cl_2. Irradiation time: (1) 0 min; (2) 8 min; (3) 30 min; (4) 75 min. (b) Spectral change on continuous irradiation. Irradiation time: (1) 75 min; (2) 127.5 min; (3) 255 min. Inset: first-order plot at 536 nm. (c) Spectral change when being kept in the dark after irradiation. Time after irradiation: (1) 0 h; (2) 18 h; (3) 100 h. Inset: second-order plot at 536 and 364 nm.

364 nm is also second-order with a k/ϵ' = (7.2 ± 1.0) × 10^{-6} s^{-1} cm. Since absorption coefficients at 536 and 364 nm were not determined in the present study, a direct comparison of the second-order rate constants at two wavelengths could be made. However, the order of the reaction is the same at both wavelengths, suggesting that the decay of band A regenerates the parent molecule. No net change was observed in the fluorescence spectrum because the fluorescence intensity, reduced during irradiation, recovered upon standing in the dark.

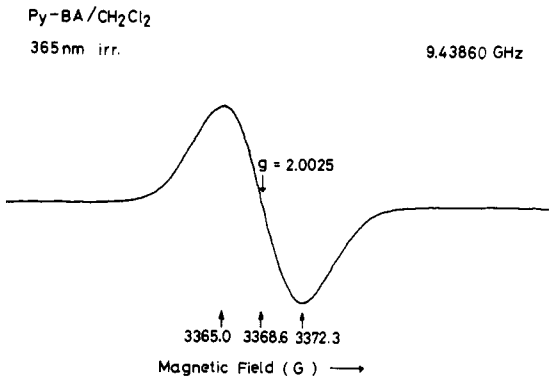

Figure 5. ESR spectrum of 1.0×10^{-2} g/L Py–BA resin in deaerated CH_2Cl_2 after 30-min irradiation at λ_{ex} = 365 nm.

Irradiated solutions (deaerated) containing A give the ESR signal (g = 2.0025; line width = 7 G) shown in Figure 5. The broad and structureless ESR spectrum provides little information about the chemical structure of the radical. Nevertheless, a strong correlation is observed between the intensities of the ESR and the optical absorption A: they both grow with irradiation time, decay similarly with prolonged irradiation, and disappear instantly upon addition of oxygen or *p*-benzoquinone. These results clearly indicate that the ESR signal and the optical absorption (band A) originate from the same species. We conclude therefore that band A is caused by a stable free radical (referred to as radical A[11]). Next we will briefly discuss the appearance of A in the other solvents.

1.3.2. Irradiation in Bz, CCl_4, and C_6H_{12}. When irradiated (λ = 365 nm) in deaerated Bz, Py–BA also yields band A (λ_{max} = 541 nm). However, the steady-state yield is only $^1/_4$ of that observed in CH_2Cl_2, assuming the same absorption coefficients. As in CH_2Cl_2, second-order kinetics are observed at both 541 nm ($2k/\epsilon = (1.5 \pm 0.8) \times 10^{-4}$ s^{-1} cm) and at 364 nm (parent species, $k/\epsilon' = (1.3 \pm 0.7) \times 10^{-5}$ s^{-1} cm). In contrast to Bz solution, radical A is not detected in CCl_4 and C_6H_{12} solutions during steady-state irradiation. In C_6H_{12}, only the consumption of the parent molecules is observed with no other major spectral change. On the other hand, in CCl_4, a quick buildup of an absorption at 380–430 nm at the expense of the parent molecules is observed.

2. Photoreaction of Py–BA with *p*-Benzoquinone (BQ). 2.1. Transient Absorption Spectrum. The fluorescence intensity and decay profile of Py–BA are strongly quenched by BQ in CH_2Cl_2 and Bz. No absorption band attributable to a ground-state charge-transfer complex is found in the presence of BQ up to 5×10^{-3} M.

Excitation with a 337-nm laser pulse in the presence of BQ (5×10^{-4} M) gives the transient spectra shown in Figure 6a in CH_2Cl_2 and in Figure 6b in Bz. The rise in the absorption is observed immediately after the excitation pulse, suggesting that the formation of the transients takes place via the S_1 state of Py–BA. The bands attributable to the triplet of Py–BA are not observed even immediately after excitation. Accordingly, radical A is considered to be responsible for the transient spectra (Figure 6a,b) regardless of the solvent. It is also found that direct excitation of BQ (e.g., [BQ] = 2×10^{-3} M) produces triplet BQ (λ_{max} = 460 nm), the subsequent decay of which is compensated by the formation of radical A.

In CH_2Cl_2, the initial radical yield observed at 540 nm in the presence of BQ is higher than that observed in the absence of BQ, but the decay of the radical is accelerated by BQ. In Bz, the formation of the radical is observed for the first time in the presence of BQ; the radical decays

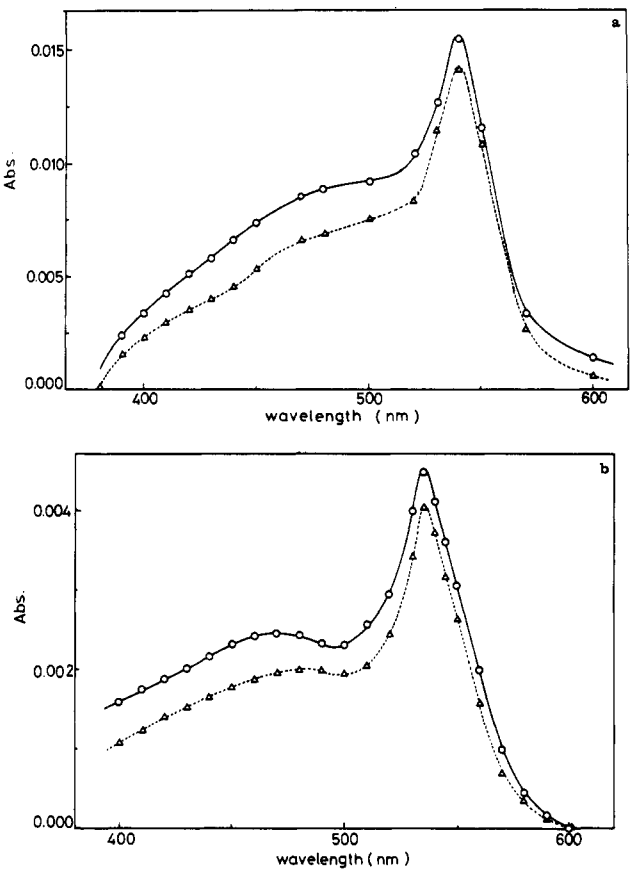

Figure 6. Transient absorption spectra of 1.5×10^{-2} g/L Py–BA resin in the presence of 5×10^{-4} M BQ. (a) In CH_2Cl_2, delay: (○) 0 μs, (△) 400 μs. (b) In Bz, delay: (○) 0 μs, (△) 450 μs.

slower in Bz than in CH_2Cl_2. It is also observed that formation of radical A takes place in C_6H_{12} in the presence of BQ; the decay at 540 nm is faster in C_6H_{12} than in Bz.

2.2. Steady-State Irradiation. 2.2.1. In CH_2Cl_2. The concentration of BQ was maintained as low as possible to minimize direct excitation of BQ. Irradiation with 365-nm light in the presence of BQ causes the buildup of absorptions at 642 and 846 nm along with the peaks at 536 and 460 nm observed in the absence of BQ (Figure 7a). Since no peaks are found in the transient spectrum, these peaks can be assigned to a product (product B) other than that produced by the direct reaction of S_1 of Py–BA with BQ. Addition of BQ (without admitting oxygen) after the formation of radical A causes the buildup of absorptions both at 642 nm and at 846 nm at the expense of the absorption of radical A, suggesting that product B is formed from radical A.

An identical spectrum to that of product B is also obtained on addition of $HClO_4$ to a CH_2Cl_2 solution of Py–BA. The redox potential of B was measured to be 0.38 V vs Ag/AgCl. This value is comparable to that of the triphenylmethyl cation (E_0 = 0.32–0.39 V vs Ag/AgCl in CH_2Cl_2) which is produced[12] on addition of $HClO_4$ to CH_2Cl_2 solutions of triphenylmethane, triphenylcarbinol, or triphenylmethyl chloride. These results strongly suggest that product B can be assigned to a triarylmethyl-type cation in analogy with a triphenylmethyl cation. In other words, radical A reacts with BQ to form a triarylmethyl-type cation (Figure 8c) in CH_2Cl_2. Participation of impurities, especially trace amounts of water, in the formation of the cation was also checked. However, both throughly dehydrated and an intentionally water-added CH_2Cl_2 solutions give the same result with regard to the cation formation. Hence, the formation of triarylmethyl cation from impurities can be ruled out.

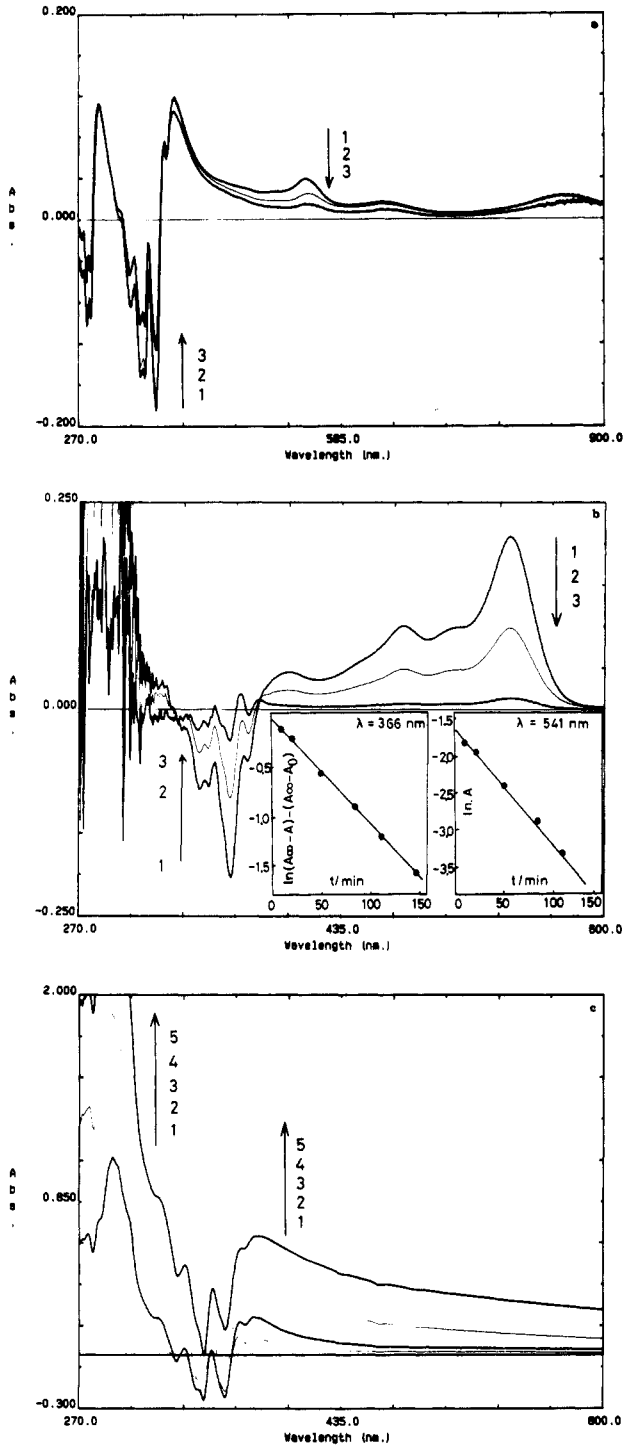

Figure 7. Difference absorption spectra on steady-state irradiation (365 nm) of 1.0×10^{-2} g/L Py–BA in the presence of BQ. (a) In CH_2Cl_2 (5×10^{-4} M BQ); irradiation time 30 s. Delay: (1) 0 min, (2) 13 min, (3) 115 min. (b) In Bz (2×10^{-3} M BQ); irradiation time 1 min. Delay: (1) 0 min, (2) 84 min, (3) 231 min. Inset, first-order plot at 541 and 366 nm. (c) In C_6H_{12}, (2×10^{-3} M BQ). Irradiation time: (1) 0 min, (2) 1 min, (3) 3 min, (4) 6 min, (5) 10 min.

In addition to the formation of triarylmethyl cation in CH_2Cl_2, a buildup is also observed at 292 nm. This peak is ascribed to the formation of hydroquinone (BQH_2), whose absorption coefficient is 2.86×10^3 M^{-1} cm^{-1} at 292 nm in CH_2Cl_2 ($\epsilon = 3.35 \times 10^2$ M^{-1} cm^{-1} for BQ at 292 nm in CH_2Cl_2). The direct excitation of BQ (without Py–BA) in CH_2Cl_2 also causes the formation of BQH_2, but with less efficiency. Therefore, care was taken to not excite BQ directly in the present Py–BA/BQ/CH_2Cl_2 system.

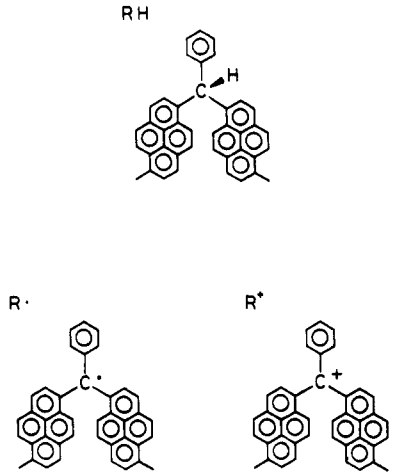

Figure 8. Structural model for triarylmethane (a), triarylmethyl radical (b), and triarylmethyl cation (c).

The examination of the reactivity of radical A toward hydroquonone (BQH_2) in CH_2Cl_2 in transient and steady-state experiments revealed that decay is enhanced in the presence of BQH_2 and the decay kinetics is no longer a simple first-order. Recovery of the parent Py–BA is observed upon reaction of radical A with BQH_2. On the other hand, the reaction of radical A with O_2 in CH_2Cl_2 obeys second-order kinetics with a rate constant of (3–7) $\times 10^5$ M^{-1} s^{-1}.[13]

2.2.2. In Benzene and in Cyclohexane. Results obtained in the presence of BQ in Bz are notably different from those in CH_2Cl_2. Irradiation at 365 nm produces radical A at the expense of the parent Py–BA absorption bands. However, radical A thus produced decays with first-order kinetics ($k = (2.3 \pm 0.4) \times 10^{-4}$ s^{-1} at 541 nm). This decay is compensated by a first-order recovery of parent Py–BA absorption bands ($k' = (1.9 \pm 0.2) \times 10^{-4}$ s^{-1} at 350 and 364 nm) as shown in Figure 7b. The two rate constants agree with each other within experimental error, indicating that the decay of radical A reproduces parent Py–BA. The recovery of the parent bands is more than 98% both at 350 nm and at 364 nm. The steady-state radical yield in Bz is 5.7 times that in CH_2Cl_2, due to the slower decay of the radical in Bz.

On the other hand, radical A is absent in the steady-state spectrum in C_6H_{12} (Figure 7c), while present in the transient spectrum. Instead, the buildup of the absorption at 292 nm, ascribable to hydroquinone (BQH_2), is significant in C_6H_{12}. This is apparently due to the hydrogen-donating nature of the solvent toward BQH·.

Discussion

1. Formation and Reaction of the Radical Site in Solution. Identification of the Radical Site. The absorption bands of radical A at ca. 540 nm and at 460 nm are ascribed to a triarylmethyl radical site (Figure 8b) produced from the triarylmethane structure (Figure 8a). This conclusion is justified by the following:

(i) The triarylmethyl radical site is the most stable among possible candidates expected from the chemical structure of the present resin due to higher resonance stabilization. The reactivity of the radical is also reminiscent of the trityl radical. The triarylmethyl radical can be transformed to the triarylmethyl cation via electron transfer and also to triarylmethane by accepting a H atom from a hydrogen donor such as hydroquinone. Our results show that radical A can be oxidized to form the triarylmethyl cation or can regenerate the parent Py–BA by reaction

Table III
Relative Radical Yield on Singlet and Triplet Quenching

solvent	relative radical yield[a] after the laser (S_1 quenching)	relative radical yield[a] T_1 quenching
C_6H_{12}	nd[b]	
Bz	nd[b,c]	
CH_2	1.0	
CCl_4	1.2	1.0[d]

[a] Relative absorbance at 535 nm. [b] Not detected. [c] Radical formation was observed on steady-state irradiation (see text). [d] 125 μs after the laser pulse.

with hydroquinone. The radical reacts with O_2 as trityl and other carbon-centered radicals do.[14]

(ii) Other possible candidates such as the radical cation of a pyrene moiety or a pyrene dimer cationic site can be excluded from spectroscopic evidence. The former should have an absorption peak at 450 nm[15] and the latter at 590 nm and in the near-IR.[16] No absorption is detected in the near-IR (900–2500 nm) region.

(iii) A proton-ENDOR spectrum[17] for a powder of irradiated Py–BA is successfully reproduced by a theoretical simulation[18] on the assumption of a triarylmethyl radical site using the spin density distribution obtained from the UHF calculation of a generalized Hubbard model. A molecular weight distribution from 3 to 6 unit structures is assumed in the calculation since the lack of a hyperfine structure in the ESR spectrum of radical A is considered to be due to inhomogeneous broadening; this phenomenon has been observed[19] for the radical sites in polymer domains.

Formation Mechanism of the Radical Site. The reaction of the Py–BA (abbreviated as RH in the reaction scheme) S_1 state is strongly dependent on the solvents used. Quenching of S_1 fluorescence is observed in Bz, CH_2Cl_2, and CCl_4 in the order of $CCl_4 > CH_2Cl_2 >$ Bz. The degree of this fluorescence quenching correlates with the solvent-dependent radical yield after the laser pulse: qualitatively speaking, a higher yield of the radical is obtained in the solvent in which a stronger fluorescence quenching is observed, as shown in Table III. This suggests that the radical formation takes place through S_1 quenching. On the other hand, as is shown in Table II, the triplet yield is not appreciably affected by the solvent used. Two possible mechanisms can be considered to operate in this quenching reaction:

(1) C–H bond homolysis from S_1

$$RH^* \rightarrow R^\bullet + H^\bullet \quad (1)$$

and (2) electron transfer to the solvent (denoted as S) followed by the proton dissociation

$$RH^* + S \rightarrow RH^+ + S^- \rightarrow R^\bullet + H^+ + S^- \quad (2)$$

Mechanism 1 is energetically possible since the excitation energy at 365 nm, 78.3 kcal/mol, is larger than the C–H bond dissociation energy, which is estimated to be substantially less than 75 kcal/mol.[20]

As far as mechanism 2 is concerned, we can estimate the free energy change (ΔG) of the singlet and triplet electron-transfer reactions (2) for CH_2Cl_2 and CCl_4 as well as BQ, as shown in Table IV. We could not measure the oxidation potential of Py–BA in CH_2Cl_2, and hence we used the literature value of pyrene. In strong electron-accepting solvents such as CCl_4, the reaction can be explained by mechanism 2 in analogy with the radical formation through reaction with BQ, because of the negative ΔG value

Table IV
Estimated Free Energy Change of the Singlet and Triplet Electron-Transfer Reactions[a]

acceptor (solvent)	$E(A/A^-)/V$[b]	$\Delta G(S_1)/eV$[c]	$\Delta G(T_1)/eV$[d]
CH_2Cl_2	−2.33	+0.27	+1.51
CCl_4	−0.78	−1.28	−0.04
BQ	−0.42	−1.64	−0.4

[a] $\Delta G = E(D^+/D) - E(A/A^-) - E(S_1)$ (or $E(T_1)$) (Kavarons, G. J.; Turro, N. J. *Chem. Rev.* **1986**, *86*, 401–449). $E(D/D^+) = 1.27$ V, $E(S_1) = 3.33$ eV, and $E(T_1) = 2.09$ eV from the same literature was employed. [b] Reduction potential of the accepter. [c] ΔG for singlet electron transfer. [d] ΔG for triplet electron transfer.

obtained both for S_1 and T_1. In CH_2Cl_2, a weak electron-acceptor, mechanism 2 is unfavorable from an energetical point of view (Table IV). In this solvent, we assume that mechanism 1 is applicable because the smaller viscosity compared with C_6H_{12} facilitates the escape of the radical and prevents cage recombination. Mechanism 1 is most likely in benzene because it lacks electron-accepting ability. It should be noted that, even in C_6H_{12}, a tiny amount of radical A is observed in the absorption spectrum after repeated laser irradiation. The reason we failed to observe radical A in the steady-state experiment is ascribed to its short lifetime in C_6H_{12}.

An appreciable difference between C_6H_{12} and Bz is seen in the S_1 quenching of Py–BA. Transient absorption spectra, however, suggest the presence of only the triplet state in both solvents. This result indicates that the yield of radical A in Bz is too small to be detected in its transient spectrum. In C_6H_{12}, the absence of S_1 quenching is ascribed to the higher viscosity.

Finally, we should mention two points. First, homolytic dissociation from the triplet state is unlikely because of the energetic requirement ($E(T_1) = \sim 48$ kcal/mol). Second, there is a possibility of dissociation due to excited-state annihilation:

$$RH(S_1^*) + RH(S_1^*) \rightarrow R^\bullet + H^\bullet + RH \quad (3)$$

$$RH(T_1^*) + RH(T_1^*) \rightarrow R^\bullet + H^\bullet + RH \quad (3')$$

However, because of the limited laser power, we could not measure the power-dependent radical yields with sufficient reliability.

Stability and Reactions of the Radical Site. The significant observation is the high yield and the long lifetime of radical A in CH_2Cl_2. Although energetically not favored, the higher yield of the radical in CH_2Cl_2 suggests the participation of mechanism 2 in addition to mechanism 1, considering that the solvent viscosity is not greatly different between CH_2Cl_2 and Bz. A higher polarity of the medium may work as a stimulus for the ionic process, i.e., mechanism 2. Due to the intrinsic stability of the radical in CH_2Cl_2, the only decay pathway is a bimolecular reaction (second-order decay, Figure 4c), probably disproportionation as shown in Figure 9.

Some remarks should be made on the observation that continuous irradiation at 365 nm after radical A is formed causes a faster decay of the latter (Figure 4b) as compared with the dark reaction. This can be explained by the reaction of the radical with the excited states of Py–BA. The consumption of parent molecules taking place during the reaction supports this explanation.

The formation of radical A is also observed in Bz under steady-state irradiation but in a low yield. A notable observation in CCl_4 is that the radical is formed from the triplet state as well as from the singlet state. This is

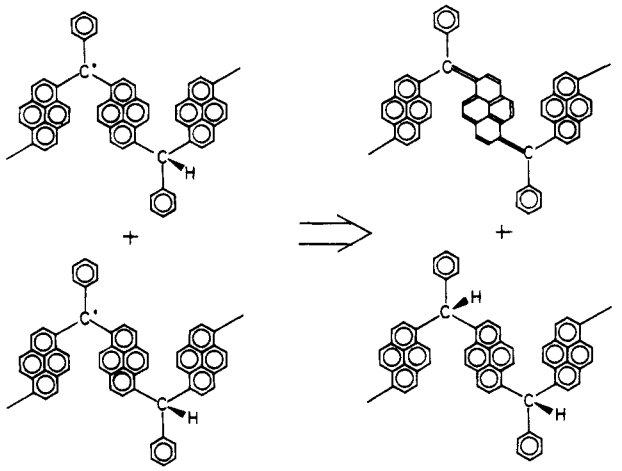

Figure 9. Reaction scheme for radical A in CH_2Cl_2.

apparently due to the high reactivity of the solvent toward the excited states. Free-energy considerations favorably support both the singlet and triplet electron-transfer mechanism (Table IV). The decay process of the radical in Bz is similar (i.e., bimolecular) to that in CH_2Cl_2. In CCl_4, on the other hand, differences in pulsed and steady-state irradiation are observed. These differences may be caused by the reaction of A with radicals such as $Cl^•$, $CCl_3^•$, and $CCl_2^{2•}$, produced from reduced solvent molecules[23] in the quenching process.

The reaction of radical A with O_2 proceeds via second-order kinetics. The observed rate constant of $k = (3–7) \times 10^5\ M^{-1}\ s^{-1}$ is significantly smaller than the rate constant for oxygenation of trityl and benzyl radicals in solution ($10^9\ M^{-1}\ s^{-1}$ [14]). Nevertheless, the reaction mechanism is ascribable to the oxygenation of radical A, because carbon-centered radicals are known to undergo oxygenation and also because another mechanism such as electron transfer is unlikely. The low rate constant is indicative of the extremely high stability of radical A and also of the steric hindrance of the polymer structure.

2. Photoreaction of Py–BA with BQ in Solution. The formation of radical A by the reaction of photoexcited Py–BA (RH*) with BQ can be explained by hydrogen abstraction (a) or electron transfer followed by deprotonation (b). The solvent polarity determines which mech-

$$RH^* + BQ \rightarrow R^• + BQH^• \quad (a)$$

$$RH^* + BQ \rightarrow RH^+ + BQ^{•-} \rightarrow R^• + H^+ + BQ^{•-} \quad (b)$$

anism is applicable. Transient absorption spectra (peaks at 540 and 460 nm) indicate that the formation of radical A occurs in all the solvents, i.e., CH_2Cl_2, Bz, or C_6H_{12}. The formation of $BQH^•$ or $BQ^{•-}$, however, is still ambiguous in the transient spectra, possibly due to their low absorption coefficients, i.e., at $\lambda_{max} = 450$ nm, $\epsilon = 6.80 \times 10^3\ M^{-1}\ cm^{-1}$ for $BQ^{•-}$ [24a] and, at $\lambda_{max} = 410$ nm, $\epsilon = 4.3 \times 10^3\ M^{-1}\ cm^{-1}$ for $BQH^•$.[24b] In the present experiment, typically 5 mJ/pulse would produce an excited-state concentration of 1×10^{-6} M. Therefore, even if a 100% efficiency is assumed, the absorbance of $BQH^•$ would be 0.004 and that of $BQ^{•-}$ would be 0.006. Accordingly, under the present experimental conditions, $BQH^•$ or $BQ^•$ would not be detected.

Strong solvent dependence is observed in the decay of the radical. First, in CH_2Cl_2, the decay is associated with the formation of a triarylmethyl cation. In the assumption of a direct oxidation mechanism by BQ

$$R^• + BQ \rightarrow R^+ + BQ^{•-} \quad (c)$$

the free energy change, ΔG, can be estimated to be

$$\Delta G = -0.38 - (-0.42) = +0.04\ V$$

where $E_0(R^•/R^+) = 0.38$ V and $E_0(BQ/BQ^{•-}) = -0.42$ V were measured in CH_2Cl_2 (vs Ag/AgCl). Accordingly, reaction c is not favorable from an energetic point of view. However, it has been reported[25] that protonated BQ is reduced at +0.2 V vs Ag/AgCl to produce hydroquinone (BQH_2). Therefore, the triarylmethyl radical formation reaction could be

$$2R^• + BQH^+ + H^+ \rightarrow 2R^+ + BQH_2 \quad (d)$$

where ΔG is then estimated to be −0.58 V ($\Delta G = -0.38 - (+0.2)$).

Second, in Bz, the decay of the radical gives rise to almost a complete recovery of the parent molecule. Mechanism a is most likely for the formation of radical A in Bz because of the nonpolar nature of the solvent. Then the $BQH^•$ produced forms BQH_2[22] by

$$BQH^• + BQH^• \rightarrow BQ + BQH_2 \quad (e)$$

and BQH_2 can give hydrogen to $R^•$:

$$BQH_2 + R^• \rightarrow BQH^• + RH \quad (f)$$

These processes explain well the observations in Bz.

Third, in C_6H_{12}, radical A must be formed in a mechanism similar to that in Bz. The reaction of $BQH^•$ with the solvent

$$BQH^• + C_6H_{12} \rightarrow BQH_2 + C_6H_{11}^• \quad (g)$$

may facilitate the accumulation of BQH_2, which is observed in the steady-state spectra. Parent Py–BA seems to degrade on continuous irradiation in C_6H_{12}. This indicates that the recovery process f is overcome by another degradation process, possibly the reaction of radical A with $C_6H_{11}^•$.

Summary

The photoreaction of a triarylmethane-type pyrene–benzaldehyde (Py–BA) resin in solution is investigated. Evidence strongly suggests the formation of a triarylmethyl-type radical site (radical A) in the resin. Radical A is shown to be significantly stable. The reactions of radical A are shown to possess features characteristic of its monomeric counterpart, i.e., a triphenylmethyl radical. The second-order decay process of radical A is ascribed to a disproportionation reaction, giving rise to the formation of a quinoid structure on the one hand and a recovery of a parent molecule on the other hand. This is due to the steric hindrance originating from a highly-disordered polymer structure. Dimerization is normally observed for the triphenylmethyl radical monomer.[27] In the photoreaction of Py–BA with *p*-benzoquinone (BQ), radical A is transformed to the triarylmethyl cation in CH_2Cl_2 and is almost completely converted back to Py–BA in benzene. Radical A reacts with oxygen; the reaction may proceed via oxygenation, although no products were identified. In the case of triphenylmethyl radicals, ditrityl peroxide is produced.[28]

Polymer-pendant triarylmethyl radicals, i.e., poly(4-vinyltriarylmethyl) radicals, have been synthesized previously,[19] and the reactivities were reported to be similar to those of the monomeric triarylmethyl radicals. This differs from the Py–BA resin where the distorted polymer

structure may hamper the normal reactivity of triarylmethyl radicals.

Currently, several attempts[29] are underway aimed at stabilizing free-radical sites in a polymer domain in order to attain a higher ordering of spins. However, the structureless ESR spectra are similar to the observation in the Py–BA resin, and only paramagnetic behavior is observed in the temperature range of 77–300 K. Therefore, at present, more research and understanding are needed in order to attain the goal of obtaining a high-spin polymer. Along this course, further studies will be conducted with the present triarylmethane resin.

Acknowledgment. This work was partly supported by a Grant-in-Aid for Science Research (No. 01750769) from the Ministry of Education, Science, and Culture, Japan. We are grateful to Professor Sugio Otani of Gunma University, Professor Masashi Imamura of the Tokyo University of Information Sciences, and Dr. Thomas W. Ebbesen of the NEC Corp. for stimulating discussions. We thank Dr. Yasumasa Hirai at KRI International, Kyoto, Japan, for his generous advice on electrochemical experiments. Thanks are also due to Dr. Takemitsu Kikuchi of Tohoku University for his help in the ESR measurements.

References and Notes

(1) (a) Ota, M.; Ota, E.; Otani, S.; Kojima, A. *J. Chem. Soc. Jpn., Chem. Ind. Chem.* **1988**, 106–113. (b) Ota, M.; Otani, S.; Kobayashi, K. *Chem. Lett.* **1989**, 1175–1178.
(2) (a) Ota, M.; Otani, S. *Chem. Lett.* **1989**, 1179–1182. (b) Ota, M.; Otani, S.; Igarashi, M. *Chem. Lett.* **1989**, 1183–1186. (c) Ota, M.; Otani, S. *Mol. Cryst. Liq. Cryst.* **1989**, *176*, 99–108. (d) Nogami, T.; Kosaka, S.; Shirota, Y.; Aota, H.; Harada, A.; Kamachi, M. *Chem. Lett.* **1989**, 1593–1596. (e) Tanaka, K.; Yamashita, S.; Yamabe, T.; Yamauchi, J.; Deguchi, Y. *Solid State Commun.* **1989**, *71*, 627–628. (f) Ota, M.; Otani, S. *Mater. Res. Soc. Symp. Proc.* **1990**, *173*, 71–76.
(3) Pryor, W. A. *Free Radicals*; McGraw-Hill: New York, 1966.
(4) Perrin, D. D.; Armarego, W. L. F. *Purification of Laboratory Chemicals*; Pergamon Press: Oxford, 1988.
(5) Hashimoto, S.; Thomas, J. K. *J. Phys. Chem.* **1985**, *89*, 2771–2777.
(6) Janata, E. *Rev. Sci. Instrum.* **1986**, *57*, 273–275.
(7) Demas, J. N. *Excited State Lifetime Measurements*; Academic Press: New York, 1983; pp 77–101.
(8) Lippert, E.; Naegel, W.; Seibold-Blankenstein, I.; Staiger, U.; Voss, W. Z. *Z. Anal. Chem.* **1959**, *170*, 1–18.
(9) Melhuish, W. H. *J. Phys. Chem.* **1961**, *65*, 229–235.
(10) Heinzelmann, W.; Labhart, H. *Chem. Phys. Lett.* **1969**, *4*, 20–24.
(11) The same ESR spectrum as that of the solution was obtained with a pink powder precipitated in methanol after Py–BA is irradiated in CH_2Cl_2 and dried in a nitrogen atmosphere; radical A is extremely stable in the powder at room temperature when kept in vacuo.
(12) (a) Chu, T. L.; Weissman, S. I. *J. Chem. Phys.* **1954**, *22*, 21–25. (b) Dauben, H. J.; Honnen, L. R.; Hamon, K. M. *J. Org. Chem.* **1960**, *25*, 1442–1445.
(13) $[O_2] = (5–10) \times 10^{-3}$ M at 25 °C, 1 atm, in CH_2Cl_2 by Hirai (private communication) is used.
(14) Millard, B.; Ingold, K. U.; Scaiano, J. C. *J. Am. Chem. Soc.* **1983**, *105*, 5095–5099.
(15) Shida, T. *Electronic Absorption Spectra of Radical Ions*; Elsevier: Amsterdam, The Netherlands, 1988; pp 85–86.
(16) Kira, A.; Imamura, M. *J. Phys. Chem.* **1979**, *83*, 2267–2273.
(17) Hashimoto, S.; Ota, M.; Takui, T., unpublished result.
(18) (a) Shichiri, T.; Teki, Y.; Takui, T.; Itoh, K. *Abstr. 2nd Japan–China Bilateral ESR Symp.* **1989**, 10–08, Japan. (b) Takui, T.; Kita, S.; Ichikawa, S.; Teki, Y.; Kinoshita, T.; Itoh, K. *Mol. Cryst. Liq. Cryst.* **1989**, *176*, 67–76.
(19) Braun, D.; Faust, R. J. *Macromol. Chem.* **1969**, *121*, 205–226.
(20) The value is estimated from the C–H bond homolytic cleavage in triphenylmethane.[21] Resonance stabilization of the present triarylmethyl moiety should be much larger than that of the triphenylmethyl radical. The homolytic photocleavage of a C–H bond was observed for triphenylmethane in EPA at 77 K[22a] and in C_6H_{12} at room temperature.[22b]
(21) Migita, T. *Radical Reactions*; Baifukan: Tokyo, 1967; p 10.
(22) (a) Porter, G.; Strachan, E. *Trans. Faraday Soc.* **1958**, *54*, 1595–1604. (b) Manring, L. E.; Peters, K. S. *J. Phys. Chem.* **1984**, *88*, 3516–3520.
(23) (a) Washio, M.; Tagawa, S.; Tabata, Y. *Radiat. Phys. Chem.* **1983**, *21*, 239–243. (b) Washio, M.; Yoshida, Y.; Hayashi, N.; Tagawa, S.; Tabata, Y. *Radiat. Phys. Chem.* **1989**, *34*, 115–120.
(24) (a) Gamage, R. S. K.; Umapathy, S.; McQuillan, A. J. *J. Electroanal. Chem.* **1990**, *284*, 229–235. (b) Patel, K. B.; Willson, R. L. *J. Chem. Soc., Faraday Trans. 1* **1973**, 814–825.
(25) Yamamoto, K.; Asada, T.; Nishide, H.; Tsuchida, E. *Bull. Chem. Soc. Jpn.* **1990**, *63*, 1211–1216.
(26) Amouyal, E.; Bensasson, R. *J. Chem. Soc., Faraday Trans. 1* **1976**, *72*, 1274–1287.
(27) Lankamp, H.; Nauta, W. Th.; MacLean, C. *Tetrahedron Lett.* **1968**, *2*, 249–254.
(28) (a) Gomberg, M. *Ber. Dtsch. Chem. Ges.* **1897**, *30*, 2043–2047. (b) Gomberg, M. *Ber. Dtsch. Chem. Ges.* **1900**, *33*, 3150–3163.
(29) (a) Nishide, H.; Yoshioka, N.; Inagaki, K.; Tsuchida, E. *Macromolecules* **1988**, *21*, 3120–3122. (b) Vlietstra, E. J.; Nolte, R. J. M.; Zwikker, J. W.; Drenth, W.; Meijer, E. W. *Macromolecules* **1990**, *23*, 946–948.

Registry No. Py–BA, 123256-55-3; *p*-benzoquinone, 106-51-4; dichloromethane, 75-09-2; cyclohexane, 110-82-7; carbon tetrachloride, 56-23-5; benzene, 71-43-2.